Enhanced Power Conversion Capability of Class-E Power Amplifiers With GaN HEMT Based on Cross-Quadrant Operation

Xianglin Hao, *Student Member, IEEE*, Jianlong Zou, Ke Yin, Xikui Ma, and Tianyu Dong, *Member, IEEE*

***Abstract*—Class-E power amplifiers are widely used in megahertz frequency power conversion systems due to their high efficiency, which can further be enhanced by virtue of wide-bandgap devices such as GaN high-electron-mobility transistors. Here, a GaN-based cross-quadrant mode Class-E amplifier is proposed, which addresses one of the major challenges for such amplifiers, i.e., to achieve both high power and high efficiency with low-voltage-rating devices. By utilizing the reverse conduction of GaN transistors, a cross-quadrant mode Class-E amplifier with small dc-feed inductance is constructed, whose circuit model is derived by virtue of the Laplace transform technique. We demonstrate an experimental prototype operating at 3.11 MHz with a 100-V GaN transistor, achieving an output power of about 6 W with the efficiency being almost 90% when the input voltage is 10 V and the load resistance is 28 Ω. Compared with conventional Class-E amplifiers, the power conversion capability of the proposed amplifier is increased up to three times from 0.49 to 1.69 with a slight reduction in efficiency. Such cross-quadrant mode amplifiers can be used to improve the power conversion capability and to reduce the peak switch voltage at the same output power level.**

***Index Terms*—Cross-quadrant mode, GaN high-electron-mobility transistors (HEMTs), radio frequency power amplifiers, resonant inverters, reverse conduction.**

I. Introduction

CLASS-E power amplifiers (PAs) or inverters [1] are radio frequency (RF) amplifiers working in resonant states. Under nominal operation, since both the zero-voltage switching (ZVS) condition and the zero-derivative switching (ZDS) condition are achieved, the elimination of the overlap between waveforms of switch current and voltage minimizes the switching losses, yielding an efficiency of 100% under ideal conditions. Since it was proposed, various aspects of the topology have been extensively investigated, including circuit tuning methods [2]–[4], loss mechanisms [5], [6], and circuit optimizations [7]–[9], to name a few.

Manuscript received 12 February 2022; revised 9 May 2022; accepted 9 June 2022. Date of publication 21 June 2022; date of current version 26 July 2022. This work was supported by the National Natural Science Foundation of China under Grant 51977165. Recommended for publication by Associate Editor D. G. Lamar. *(Corresponding author: Tianyu Dong.)*

The authors are with the School of Electrical Engineering, Xi'an Jiaotong University, Xi'an 710049, China (e-mail: z22105165@stu.xjtu.edu.cn; superzou@mail.xjtu.edu.cn; yinke2018@stu.xjtu.edu.cn; maxikui@mail.xjtu.edu.cn; tydong@mail.xjtu.edu.cn).

Color versions of one or more figures in this article are available at https://doi.org/10.1109/TPEL.2022.3184952.

Digital Object Identifier 10.1109/TPEL.2022.3184952

In recent years, considerable interests in Class-E PAs have been remanifested due to the emergence of new semiconductor power devices and the demand of fascinating applications that require high-efficiency PAs, e.g., wireless communications [10] and wireless power transmissions (WPTs) [11]–[17]. In the emerging applications of parity-time symmetric WPT [18]–[20], inverters with both the high frequency and high efficiency are typically required. Although conventional Class-E amplifiers may meet such demands [19], their output capability is not high enough, which limits the improvement of the output power as well as the power density of the entire WPT system. Therefore, it is becoming a key issue to improve the output power of Class-E PAs in WPT systems.

For resonant converters such as Class-E amplifiers, conventional designs may have great limitations when they are used to improve the output power, e.g., by increasing the duty cycle or the input voltage. When the duty cycle is increased, the peak switch voltage of the transistor will be increased [4], implicating that expensive transistors may be required. As for directly increasing the input voltage, it often requires a power transistor with higher voltage ratings, which will also increase the cost. Therefore, one of the main challenges for Class-E PAs is still to improve the *so-called power conversion capability*, namely, the ability to achieve a higher output power while the load and input voltage remain unchanged.

When optimizing a Class-E amplifier, one often needs to change the switching conditions. The off-nominal design (i.e., no ZDS condition but only the ZVS condition is achieved) for Class-E PAs has been studied [3], [12]. In addition, a design method of Class-E amplifier with variable voltage switching conditions was presented [3], [21]. Although many efforts have been devoted to study nonideal switching conditions of Class-E amplifiers [8], [22], switches are still limited to operate in the first quadrant, i.e., both switching voltage and current are greater than or equal to zero, which seems unreasonable nowadays as new bidirectional devices continue to appear. It is noted that the reverse conduction caused by the MOSFET body diode effect has been analyzed in [23]. Unfortunately, it is not considered a usable design method.

In this article, we utilize the reverse conduction of GaN high-electron-mobility transistors (HEMTs) in Class-E PAs and demonstrate that the cross-quadrant operation can, in principle, enhance the power conversion capability. Moreover, we propose a cross-quadrant mode Class-E PA, which is basically an

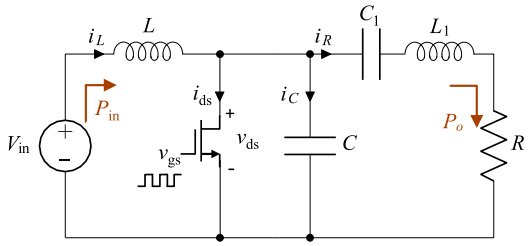

Fig. 1. Circuit schematic of a single-ended Class-E PA.

off-nominal operation amplifier under a reverse conduction switching condition. Our study not only enriches resonant inverter families and provides new design strategies for megahertz-frequency GaN-HEMT-based Class-E PAs, but also paves a pathway to utilize the reverse conduction of transistors in power converter circuits. We note that although this article will only focus on the cross-quadrant operation of GaN HEMTs for Class-E PAs, the proposed design procedure and mathematical equations can be readily applied to amplifiers made with other bidirectional devices, including silicon (Si) and silicon carbide (SiC) devices.

II. Methods for Power Conversion Capability Enhancement

A. Power Conversion Capability

Unlike applications in the area of wireless communication, when PAs are designed as inverters, the output power rather than the power gain becomes more important; however, there is still a lack of widely accepted parameter when evaluating the power output performance of the inverter topology. Toward this end, normalized output power K_P reported in [4] and [7] can be used to quantify the output power performance. To clarify the actual physical significance of this indicator, we would prefer the terminology *power conversion capability* hereafter.

For the single-transistor Class-E amplifier shown in Fig. 1, the power conversion capability can be expressed as

$$K_P = \frac{P_o R}{V_{\text{in}}^2} \tag{1}$$

where P_o is the output power, R is the load resistance, and V_{in} is the dc input voltage. The normalized output power K_P reflects the output power when the input voltage is 1 V and the load resistance is 1 Ω. Hereafter, we would refer to K_P as the *power conversion capability*. For a given load R and an input voltage V_{in}, the larger the power conversion capability, the greater the ac power output of the amplifier. Therefore, it can be a very useful indicator to characterize the performance of power inverters.

For Class-E PAs, the output power of each load satisfies $P_o = K_P V_{\text{in}}^2/R$, implying that K_P is one of the key parameters that determine the output power. If K_P can be increased, a high output power can be obtained. Owing to the use of RF chokes, the power conversion capability K_P is 0.5768 in the original Class-E circuit designed by Sokal and Sokal [24]. However, for Class-E PAs with finite dc-feed inductance, it has been shown that K_P is a function of q, where $q = 1/(\omega\sqrt{LC})$ is the ratio of the resonant frequency of the bypass resonant tank (L, C) to the operating frequency ω [1], [4], [7], [25]. Specifically, when q is relatively large, K_P is quite small (even less than 0.5768), which means that the RF output power from a certain dc input voltage is far from the limit. Thus, considerable room exists for the improvement of the maximum output power of conventional Class-E PAs. Moreover, we aim to further extend the design strategies of off-nominal Class-E PAs to achieve high maximum power, which cannot be realized by simply adjusting the effective load resistance via matching networks.

When investigating a Class-E PA operating under the duty cycle D, one typically assumes that load current is $i_R = I_R \sin(\omega t + \varphi)$, with I_R being the amplitude of the load current and φ denoting the initial phase. Since the output power reads $P_o = V_R^2/(2R)$, with $V_R = I_R R$ being the voltage (amplitude) across the load resistance, the power conversion capability K_P can be rewritten as

$$K_P = \frac{1}{2}\left(\frac{V_R}{V_{\text{in}}}\right)^2 \tag{2}$$

implying that it is determined by the ratio of the output to the input voltage, i.e., V_R/V_{in}, for single-frequency output. If the transistor were an ideal switch, the input power is equal to the output power, i.e., $P_{\text{in}} = P_o$. Considering that $P_o = V_R I_R/2$ and $P_{\text{in}} = V_{\text{in}} I_{\text{in}}$, where I_{in} is the mean value of the input current i_L, i.e., $I_{\text{in}} = \frac{1}{2\pi}\int_0^{2\pi} i_L(\omega t) d(\omega t)$, we have

$$\frac{V_R}{V_{\text{in}}} = \frac{2I_{\text{in}}}{I_R}. \tag{3}$$

Since the amplitude of i_R, i.e., I_R, should be greater than I_{in}, according to [26], we can obtain that $0 < V_R/V_{\text{in}} < 2$ and $0 < K_P < 2$, which implies that the maximum power conversion capability of a Class-E amplifier can be close up to 2. However, for conventional Class-E PAs, the power conversion capability K_P is determined by the duty cycle D and q. Most Class-E amplifier works at a 50% duty cycle, whose maximum power conversion capability is only 1.365 [1], [7], [25]. Moreover, such a maximum can only be achieved when the impedance X of the series resonant tank (L_1, C_1) is zero when q is limited to a fixed value. As a result, we expect to further enhance the power conversion capability by increasing the output voltage V_R. Our work is equivalent to optimizing the circuit design for higher V_R. Note that V_R is the voltage division of the fundamental frequency component of v_{ds} on the load resistance; thus, in order to increase V_R, the waveform of v_{ds} must be further optimized, which can be achieved by adjusting the operating mode of the transistor.

B. Cross-Quadrant Operation

In order to improve the power conversion capability of Class-E PAs in a wide range of q, we introduce the so-called cross-quadrant operation to increase the effective ON-time of the transistor, while the duty cycle of the gate control signal remains unchanged.

In conventional amplifiers, it is usually assumed that the transistor works in the first quadrant, while the reverse conduction is only considered as a special operating condition. In contrast, when a PA operates in the cross-quadrant operation, the

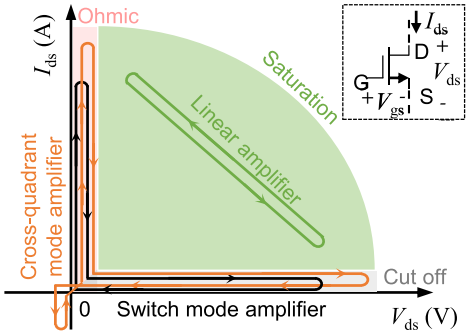

Fig. 2. Parametric space between the drain-to-source voltage (V_{ds}) and drain current (I_{ds}). Different transistor operating regimes are illustrated in the shading areas, i.e., saturation (light green), ohmic (orange), and cutoff (gray) regimes. Contours represent various modes, namely, linear (green), switch (black), and cross-quadrant (orange) modes.

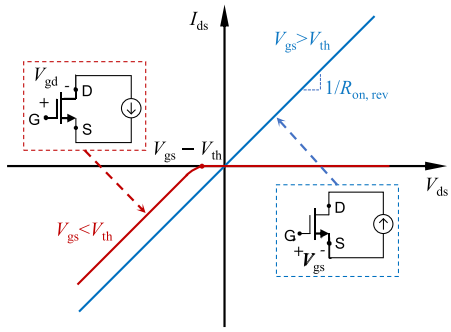

Fig. 3. Simplified conductive behavior and characteristics of the GaN HEMT in the first and third quadrants. The blue and red curves are for the forward and reverse conduction, respectively.

transistor is not limited to operate in any particular quadrant, and the design space is extended to the entire phase space spanned by drain–source voltage and current. Fig. 2 displays different operating regimes of transistors. In addition, the simplified operating trajectories of different types of amplifiers are illustrated. Transistors operate in the first quadrant for linear and conventional switch-mode amplifiers. In a linear amplifier, transistors would possess both high drain current (I_{ds}) and drain–source voltage (V_{ds}) during the majority of the period. As a result, high conduction losses appear, which is not beneficial to efficiency-demanding applications. Although amplifiers operating at the switch mode yield a near-unity efficiency, they often have limited power conversion capability.

Different from the conventional amplifiers, amplifiers working in the cross-quadrant mode allow transistors to operate alternately in the first or the third quadrant for the ON state, or in the OFF state. In order to achieve higher power conversion capability, transistors should terminate the switch-OFF state in advance and turn in the reverse conduction state, implicating that a larger effective ON-time is presented. We stress that such a feature is essentially different from that by increasing the duty cycle. In fact, since negative drain–source voltage and current are introduced within the cross-quadrant operation, the system can have a higher ac component output under the same dc input voltage.

C. Reverse Conduction Characteristics of GaN Devices

Cross-quadrant operation requires the transistors to be bidirectional switches. For high-frequency applications such as WPT systems, GaN devices are prominent because they allow for reverse current conduction, high voltage breakdown, and high switching frequency as the switch of the proposed Class-E PA. Prior to the circuit design, it is necessary to clarify the reverse characteristics of the device. Commercial GaN power transistors are mainly HEMTs, which have quite different reverse conduction characteristics, compared with Si/SiC-based MOSFETs that are well known for its reverse conduction characteristics due to the bulk diode [27]. The conductive channel of GaN HEMTs is mainly comprised of a source and a drain, which are connected by two-dimensional electron gases (2DEGs). The 2DEGs form a native channel between the source and the drain of the device, whose conductivity is controlled by the gate voltage. The conductive channel region between the source and the drain in GaN HEMTs is geometrical symmetric [28]. In the third-quadrant ($V_{ds} < 0$), the drain and source terminals can swap termination. Despite that a GaN HEMT does not have a body diode, it still presents the so-called self-commutated reverse conduction characteristics or diode-like behaviors but with zero reverse recovery loss [28].

Fig. 3 illustrates the simplified output characteristic of GaN enhancement-mode devices in the first and third quadrants. The channel turns ON in the forward conduction when the gate–source voltage V_{gs} exceeds its threshold V_{th} or in the reverse direction (third quadrant) when the gate–drain voltage V_{gd} exceeds the threshold voltage $V_{gd,th}$. During the reverse conduction state, the gate–drain voltage $V_{gd} = V_{gs} + V_{sd}$ is slightly smaller than the threshold voltage V_{th}, enabling the reverse current I_{sd} flowing through the channel. As a result, the voltage drop between the drain and the source reads

$$V_{ds} = V_{gs} - V_{gd,th} - I_{ds}R_{on,\,rev} \tag{4}$$

where $R_{on,\,rev}$ is the equivalent ON-resistance in the third quadrant and $V_{gd,th}$ is usually written as V_{SD} in the datasheet.

Due to the zero reverse recovery loss and the self-commutated reverse conduction characteristic, the cross-quadrant operation of the field-effect transistor is feasible, which provides a new degree of freedom for the design of resonant converters. By using GaN devices, the cross-quadrant operation only introduces additional reverse conduction and switching losses, where the reverse conduction loss is dominant. We shall point out that the source-to-drain voltage drop in GaN devices during the reverse conduction is much greater than that in a Si MOSFET body diode [28].

III. Theoretical Analysis and Modeling

A. Circuit Modeling of Cross-Quadrant Mode Class-E PA

Fig. 4(a) and (b) displays the waveforms of the switch voltage and current in the conventional and the cross-quadrant mode Class-E amplifiers, respectively. In the conventional analysis, switches are considered to have only two states [2], i.e., ON or

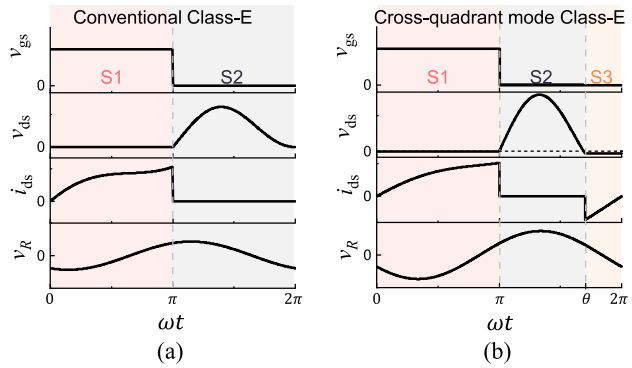

Fig. 4. Optimal waveforms of gate voltage (v_{gs}), drain-to-source voltage (v_{ds}), drain current (i_{ds}), and load voltage (v_R) for (a) the conventional Class-E PAs and (b) cross-quadrant mode Class-E PAs, when $q = 1.7$.

OFF. However, for Class-E amplifiers based on a bidirectional switch, the switch may have three states from a physical perspective, namely, switch-ON, switch-OFF, and reverse conduction, respectively. By properly designing the circuit parameters, one can control the transistor reverse conduction at a specific time without changing the driving signal and realize the cross-quadrant operation.

Fig. 4(b) illustrates the switching behaviors and states for the considered cross-quadrant mode Class-E PAs. Here, we assume that the switching frequency ω_0 and operating frequency ω are equal, i.e., $\omega_0 = \omega$, and adopt a duty ratio of 50% for the gate voltage V_{gs}, where the switch action is considered to be instantaneous. The switch is ON during $0 \le \omega t < \pi$ and OFF during $\pi \le \omega t < \theta$, while it becomes reverse conductive during $\theta \le \omega t < 2\pi$. The proposed cross-quadrant Class-E amplifier is basically a conventional off-nominal one. In the cross-quadrant amplifier, $v_{ds}(\theta) = -V_{SD}$, while $v_{ds}(2\pi) = 0$ in an off-nominal Class-E amplifier despite that ZDS is not achieved. To simplify the analysis hereafter, we assume that the GaN HEMT has an infinite OFF-state resistance and the ON-resistance is small enough, which would not affect the voltage waveform.

Next, we focus on the detailed analysis of the three states of the Class-E circuit illustrated in Fig. 1. The aim is to derive the expressions of the switch current i_{ds} and voltage drop v_{ds} between the drain and source, so that we can design a better tuning method.

1) Switch ON ($0 \le \omega t < \pi$): When the switch is ON, the voltage drop on the switch reads

$$v_{ds}(\omega t) = V_{in} - v_L(\omega t) = 0. \tag{5}$$

In addition, the switch current reads $i_{ds}(\omega t) = i_L(\omega t) - i_R(\omega t) - i_C(\omega t)$ with $i_L(\omega t) = i_L(0) + (\omega L)^{-1}\int_0^{\omega t} V_{in}\mathrm{d}(\omega t) = i_L(0) + \omega t V_{in}/(\omega L)$ and $i_C(\omega t) = \omega C\frac{\mathrm{d}v_{ds}(\omega t)}{\mathrm{d}(\omega t)} = 0$, where $C = C_{ext} + C_{oss}$ denotes the total parallel capacitance, with C_{oss} being the transistor's parasitic output capacitance and C_{ext} being the external shunt capacitance. As a result, the switch current i_{ds} can be rewritten as

$$i_{ds}(\omega t) = \frac{V_{in}}{\omega L}\omega t + i_L(0) - I_R\sin(\omega t + \varphi). \tag{6}$$

2) Switch OFF ($\pi \le \omega t < \theta$): When the switch is OFF, no current flows through the switch, i.e.,

$$i_{ds}(\pi \le \omega t < \theta) = 0. \tag{7}$$

Now, the shunt capacitor current reads $i_C(\omega t) = i_L(\omega t) - i_R(\omega t) = (\omega L)^{-1}\int_{\pi}^{\omega t}[V_{in} - v_{ds}(\omega t)]\mathrm{d}(\omega t) + i_L(\pi) - I_R\sin(\omega t + \varphi)$. Alternatively, considering $i_C(\omega t) = \omega C\frac{\mathrm{d}v_{ds}(\omega t)}{\mathrm{d}(\omega t)}$, one can derive a nonhomogeneous second-order linear differential equation [7], [25], [29], which reads

$$\omega^2 LC\frac{\mathrm{d}^2 v_{ds}(\omega t)}{\mathrm{d}(\omega t)^2} + v_{ds}(\omega t) - V_{in} + \omega L I_R\cos(\omega t + \varphi) = 0. \tag{8}$$

Solving the ordinary differential equation (8), one would arrive at the solution to the switch voltage v_{ds} normalized to the input voltage V_{in} as

$$\frac{v_{ds}(\omega t)}{V_{in}} = 1 - A_1\cos(q\omega t) + A_2\sin(q\omega t) + \frac{q^2 p}{1-q^2}\cos(\omega t + \varphi) \tag{9}$$

where $q = 1/(\omega\sqrt{LC})$ and $p = \omega L I_R/V_{in}$ are regarded as design parameters; the coefficients A_1 and A_2 can be determined with certain initial conditions.

If we assume that the initial switch current satisfies

$$i_{ds}(0) = kI_R \tag{10}$$

where the design parameter k denotes the proportional coefficient between the initial switch current $i_{ds}(0)$ and the load current I_R, the coefficients A_1 and A_2 can be determined from the initial OFF-state conditions as

$$A_1 = q(\pi + kp)\sin(q\pi) + \cos(q\pi) + \xi_+ \tag{11}$$

$$A_2 = q(\pi + kp)\cos(q\pi) - \sin(q\pi) - \xi_- \tag{12}$$

with $\xi_\pm = \frac{pq}{q^2-1}[q\cos\varphi\cos(q\pi) \mp (1-2q^2)\sin\varphi\sin(q\pi)]$.

3) Reverse Conduction ($\theta \le \omega t < 2\pi$): The switch turns ON in the reverse direction when the gate-drain voltage $V_{gd} = V_{gs} + V_{sd}$ exceeds the threshold voltage $V_{gd,th}$[28]. It operates in the third quadrant during this period and has a negative current while $v_{gs} = 0$. In addition, the reverse voltage is a function of the reverse current according to (4). In this scenario, the circuit behaves as a second-order system. However, since the discharging process of C is suppressed and the reverse conduction resistance $R_{on,\,rev}$ is small (just a few tens of milliohms), the switch drain–source voltage v_{ds} would only slightly vary around the reverse conduction voltage, which can be approximated as

$$v_{ds}(\omega t) = -V_{SD} \tag{13}$$

with V_{SD} being the reverse conduction threshold voltage of the GaN device, which is usually given in the datasheet.

As for the current flowing through the switch, it can be derived as

$$i_{ds}(\omega t) = \frac{V_{in} + V_{SD}}{\omega L}(\omega t - \theta) + i_L(\theta) - I_R\sin(\omega t + \varphi). \tag{14}$$

B. Model Solving and Optimization

According to the reverse conduction conditions of GaN devices, the drain–source voltage at the end of the OFF state satisfies $v_{\rm ds}(\theta) = -V_{\rm SD}$. In addition, the switch current should be zero when $\omega t = 0$ to avoid the oscillation of the switch voltage during the switching process; thus, the design parameter k should be zero in (10) so that $i_{\rm ds}(0) = 0$. In summary, the switching conditions of the Class-E amplifier operating in the cross-quadrant mode are

$$\begin{cases} v_{\rm ds}(\theta) = -V_{\rm SD} & \text{(15a)} \\ i_{\rm ds}(0) = 0. & \text{(15b)} \end{cases}$$

We next shift to directly derive the circuit parameters when the maximum power conversion capability is achieved. Since the power conversion capability reads $K_P = V_R^2/(2V_{\rm in}^2)$, we aim to achieve high output voltage V_R with given input voltage $V_{\rm in}$. From the ω-component of the switch drain–source voltage

$$v_{{\rm ds},\omega}(\omega t) = V_R \sin(\omega t + \varphi) + V_X \cos(\omega t + \varphi) \tag{16}$$

where V_X is the voltage amplitude across the impedance X of the series resonant tank (L_1, C_1), we can obtain the output voltage V_R according to the Fourier transform [14], which reads

$$V_R = \frac{1}{\pi}\int_0^{2\pi} v_{\rm ds}(\omega t)\sin(\omega t + \varphi){\rm d}(\omega t). \tag{17}$$

Substituting (5), (9), and (13) into (17), one can express V_R as

$$V_R = \frac{V_{\rm in}}{\pi(1-q^2)}\left[A_3 + qA_4 + \frac{pq^2}{2}\sin\theta\sin(\theta+2\varphi)\right] + \frac{V_{\rm SD}-V_{\rm in}}{\pi}\cos\varphi - \frac{V_{\rm SD}+V_{\rm in}}{\pi}\cos(\theta+\varphi) \tag{18}$$

where $A_3 = [A_1\cos(q\pi) - A_2\sin(q\pi)]\cos\varphi + [A_1\cos(q\theta) - A_2\sin(q\theta)]\cos(\theta+\varphi)$ and $A_4 = [A_1\sin(q\pi) + A_2\cos(q\pi)]\sin\varphi + [A_1\sin(q\theta) + A_2\cos(q\theta)]\sin(\theta+\varphi)$, with A_1 and A_2 given in (11) and (12), respectively. Since $k = 0$, according to cross-quadrant mode switching condition (15b), the output voltage V_R is now a function with respect to the parameters p, q, θ, and φ. We shall note that $V_R = V_R(p, q, \theta, \varphi)$ is an implicit function since $p = \omega L I_R/V_{\rm in} = \omega L R^{-1} V_R/V_{\rm in}$ depends on V_R. Finally, one obtains

$$K_P(p, q, \theta, \varphi) = \frac{V_R(p, q, \theta, \varphi)^2}{2V_{\rm in}^2}. \tag{19}$$

It is evident that the greater the output voltage V_R, the greater the power conversion capability K_P. Therefore, for a specific design parameter of q, one can obtain the maximum power conversion capability by solving the following optimization problem:

$$\begin{aligned} &\max \quad V_R(p, \theta, \varphi) \\ &\text{s.t.} \quad p > 0, \quad \theta \in [\pi, 2\pi], \quad \varphi \in [0, 2\pi]. \end{aligned} \tag{20}$$

Accordingly, the corresponding parameters p, θ, and φ are derived for the maximum of V_R (or equivalently K_P). The above multivariate nonlinear optimization problem (20) can be readily handled by various optimization algorithms. For instance, this problem can be converted into finding the minimum of $-V_R$ and be solved by using the optimization toolbox (e.g., *fmincon* function) in MATLAB. Note that proper upper bound for p is required to avoid local solutions, which can be equal to the corresponding p value of the conventional Class-E PAs. Having determined the output voltage amplitude V_R, we can further obtain other derived performance parameters of the cross-quadrant mode Class-E amplifier, e.g., the efficiency, the optimal load resistance, and the voltage stress, which are discussed in the following.

C. Performance Parameters

1) Power Loss and Efficiency: In Section II-C, we have indicated that the reverse conduction loss can be the main source. Since the ON-resistance is not considered for simplicity, one can use the reverse voltage and current to estimate the reverse conduction losses. Within the cross-quadrant operation, additional reverse conduction loss power reads

$$P_{\rm rc} = \frac{V_{\rm SD}}{2\pi}\int_\theta^{2\pi} i_{\rm ds}(\omega t){\rm d}(\omega t) \tag{21}$$

where $i_{\rm ds}$ is given in (14). As a result

$$P_{\rm rc} = \frac{\alpha V_{\rm SD} I_R}{2\pi p} \tag{22}$$

where $\alpha = (1 + V_{\rm SD}/V_{\rm in})(2\pi^2 + \theta^2/2 + \theta - 2\pi) + (A_5 + \pi)(2\pi - \theta) + p[\cos\varphi - \cos(\theta+\varphi) + (2\pi - \theta)\sin\varphi]$ with $A_5 = A_1[\sin(q\pi) - \sin(q\theta)]/q + A_2[\cos(q\theta) - \cos(q\pi)]/q + q^2 p[\sin(\theta+\varphi) + \sin\varphi]/(q^2-1)$. Now, since the ZVS condition is not satisfied, switching losses are introduced, which can be expressed as

$$P_{\rm sw} = \frac{1}{4\pi}\omega C V_{SD}^2 = \frac{I_R V_{\rm SD}^2}{4\pi q^2 p V_{\rm in}}. \tag{23}$$

It is evident that both of the losses are acceptable when $V_{\rm SD}$ is small. In practice, one can choose devices with suitable $V_{\rm SD}$ to meet power loss requirements. Furthermore, advanced drive technologies are expected to effectively reduce the reverse conduction losses [30], [31].

When the power loss caused by the ON-resistance of the transistor is negligible, the efficiency η can be calculated as

$$\eta = 1 - \frac{P_{\rm rc}}{P_{\rm in}} - \frac{P_{\rm sw}}{P_{\rm in}} \tag{24}$$

with $P_{\rm in} = V_{\rm in} I_{\rm in}$, where the input current $I_{\rm in}$ can be calculated by integrating the drain current $i_{\rm ds}(\omega t)$ over a period, namely, $I_{\rm in} = \frac{1}{2\pi}\int_0^{2\pi} i_{\rm ds}(\omega t)d(\omega t)$. According to (22)–(24), we obtain

$$\eta = 1 - \frac{\alpha}{\beta}\frac{V_{\rm SD}}{V_{\rm in}} - \frac{1}{2\beta}\left(\frac{V_{\rm SD}}{qV_{\rm in}}\right)^2 \tag{25}$$

where $\beta = (1 + V_{\rm SD}/V_{\rm in})(2\pi - \theta)^2/2 + (A_5 + \pi)(2\pi - \theta) + \pi^2/2 + p[-\cos\varphi - \cos(\theta+\varphi) + (3\pi - \theta)\sin\varphi]$.

2) Voltage and Current Stresses: As illustrated in Fig. 4, the maximum of the switch voltage during the switch-OFF period is the peak drain–source voltage $V_{\rm DSM}$. Assuming that $\omega t = \phi_v$ (with $\pi < \phi_v < \theta$) when the switch voltage $v_{\rm ds}$ is the maximum,

the derivative of the switch voltage should be zero, i.e.,

$$\left.\frac{\mathrm{d}v_{\mathrm{ds}}(\omega t)}{\mathrm{d}(\omega t)}\right|_{\omega t=\phi_v} = 0 \tag{26}$$

with $v_{\mathrm{ds}}(\omega t)$ given in (9), from which one can readily obtain ϕ_v and the peak drain–source voltage $V_{\mathrm{DSM}} = v_{\mathrm{ds}}(\phi_v)$. As a result, the voltage stress is

$$\sigma_V = V_{\mathrm{DSM}}/V_{\mathrm{in}}. \tag{27}$$

Voltage stress provides an intuitive estimate of how close the peak in the drain voltage waveform is to the transistor breakdown voltage value, which is significant for reflecting device reliability. However, such an indicator does not reflect the cost of output power. When deploying realistic transistors in a Class-E amplifier circuit, the peak drain–source voltage per watt of the output power, i.e., V_{DSM}/P_o, may be a good additional indicator for estimating the cost of power. Transistors with low voltage ratings can be used when V_{DSM}/P_o is small, implying that the cost per watt of output power is low. According to (1), the normalized voltage stress, defined as

$$\tilde{\sigma}_V = V_{\mathrm{DSM}}/(V_{\mathrm{in}}K_P) \tag{28}$$

is equivalent to V_{DSM}/P_o (note that $\tilde{\sigma}_V = V_{\mathrm{DSM}}V_{\mathrm{in}}/(P_oR)$, while V_{in}/R is constant), which can be used to characterize the performance of the amplifier.

As for the current stress σ_I, it reads as

$$\sigma_I = \frac{I_{\mathrm{DM}}}{I_{\mathrm{in}}} \tag{29}$$

where I_{DM} is the peak current, which may appear when (i) $di_{\mathrm{ds}}(\omega t)/(dt) = 0$; ii) $\omega t = \pi$; iii) $\omega t = \theta$; or iv) $\omega t = 2\pi$. For case (i), if we assume that the derivative of the switch current is zero when $\omega t = \phi_i$, one arrives at $I_{\mathrm{DM}}^{\mathrm{I}} = i_{\mathrm{ds}}(\phi_i)$. For case (ii), since no peaks appear in the drain current, I_{DM} that may appear when $p < 1$ reads as $I_{\mathrm{DM}}^{\mathrm{II}} = i_{\mathrm{ds}}(\pi) = \pi V_{\mathrm{in}}/(\omega L) + i_L(0) - I_R\sin(\pi+\varphi)$, according to (6), which can further be simplified to $I_{\mathrm{DM}}^{\mathrm{II}} = (\pi/p + 2\sin\varphi)I_R$. For cases (iii) and (iv), we have $I_{\mathrm{DM}}^{\mathrm{III}} = i_{\mathrm{ds}}(\theta)$ and $I_{\mathrm{DM}}^{\mathrm{IV}} = i_{\mathrm{ds}}(2\pi)$, respectively. In summary, the peak current should be $I_{\mathrm{DM}} = \max(I_{\mathrm{DM}}^{\mathrm{I}}, I_{\mathrm{DM}}^{\mathrm{II}}, I_{\mathrm{DM}}^{\mathrm{III}}, I_{\mathrm{DM}}^{\mathrm{IV}})$.

3) Maximum Operating Frequency: At high frequencies, the output capacitance C_o of a transistor should be greater than the shunt capacitance C in order to satisfy the switching conditions [1]. The maximum operating frequency $f_{\max}$ of a Class-E PA is reflected by the design parameter $K_C = \omega CR$ introduced in [7], which describes the relationship between frequency ω, load resistance R, and switch shunt capacitance C. Therefore, $f_{\max} = \frac{K_C}{2\pi C_o R}$ when $C = C_o$, where $K_C = V_R/(q^2pV_{\mathrm{in}})$. Moreover, when the optimal load resistance $R_{\mathrm{opt}} = K_PV_{\mathrm{in}}^2/P_o$ is adopted, the maximum operating frequency reads

$$f_{\max} = \frac{K_CP_o}{2\pi C_oK_PV_{\mathrm{in}}^2}. \tag{30}$$

IV. Performance Comparison and Analysis

Fig. 5(a)–(c) shows the power conversion capability K_P, efficiency η, and initial phase shift φ with respect to the parameter q, respectively, both for the proposed and the conventional

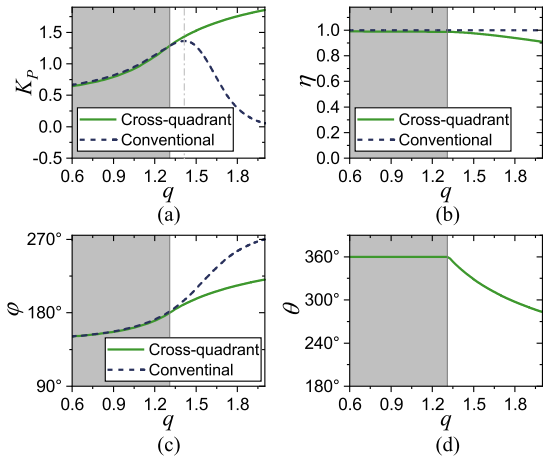

Fig. 5. (a) Normalized output power, (b) efficiency, and (c) initial phase shift φ for the conventional Class-E PAs with finite dc-feed inductance (dashed lines) and the proposed GaN-based cross-quadrant mode Class-E PAs (solid lines). (d) Reverse conduction angle θ as a function of q for the proposed GaN-based cross-quadrant mode Class-E PAs. In the analysis, the input voltage is $V_{\mathrm{in}} = 10$ V and the reverse voltage is $V_{\mathrm{SD}} = 1.7$ V. The duty ratio is 50%. For conventional Class-E amplifiers, the nominal operation is assured for each value of q.

amplifiers. It can be seen that the initial phases φ for the two amplifiers are almost the same when $q \leq 1.31$ and differ when $q > 1.31$, indicating that the cross-quadrant mode Class-E PA is reduced to the conventional one when the parameter q is small ($q \leq 1.31$), while it becomes effective when q is relatively large. Fig. 5(d) shows the reverse conduction angle θ with respect to the parameter q for the proposed amplifiers. Again, θ nearly equals 360° when the parameter q is small ($q \leq 1.3$), and it will be decreased as the value of q is increased when $q > 1.31$. In addition, the power conversion capability is monotonically increased as q is increased for the proposed PA, while it has a local maximum at $q = 1.412$ for the conventional one [see gray-dotted line in Fig. 5(a)]. The power conversion capability can be enhanced within the proposed Class-E PA that works in the cross-quadrant mode when $q > 1.31$, implicating that a high maximum output power is achieved.

Since the optimum resistance reads $R_{\mathrm{opt}} = K_PV_{\mathrm{in}}^2/P_o$, according to (1), it is proportional to $K_P(q)$. Therefore, for a certain input voltage and output power, the optimal load resistance R_{opt} for the cross-quadrant mode is greater than that of the conventional one. In RF applications, the optimal resistance of Class-E is usually much smaller than the standard load of 50 Ω [1], [25]; a larger optimal resistance is easier to match to the standard load. Thanks to the larger optimum load resistance, the switching current of the cross-quadrant mode Class-E amplifier is smaller for the same output power. Consequently, the losses caused by the ON-resistance of the switch can be small, which can partially offset the efficiency reduction caused by reverse conduction.

It is known that the inductance (capacitance) of an inductor (capacitor) depends on its size, i.e., the larger the inductor (capacitor), the greater the inductance (capacitance). Consequently, the parameter $q = (\omega\sqrt{LC})^{-1}$ will be decreased when the inductance (capacitance) is increased (equivalently the size

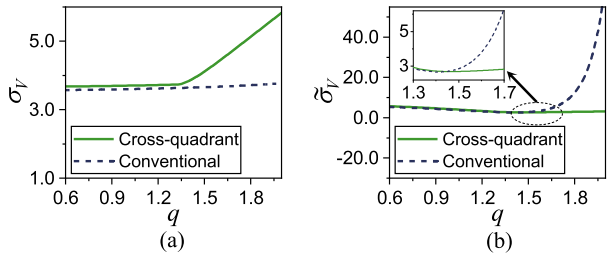

Fig. 6. (a) Voltage stress ($\sigma_V = V_{\rm DSM}/V_{\rm in}$) and (b) normalized voltage stress ($\tilde{\sigma}_V = V_{\rm DSM}/(V_{\rm in}K_P)$) for the conventional (dashed curves) and proposed cross-quadrant mode (solid curves) Class-E amplifiers. In the analysis, the input voltage is $V_{\rm in} = 10$ V and the reverse voltage is $V_{\rm SD} = 1.7$ V. The duty ratio is 50%. For conventional Class-E amplifiers, the nominal operation is assured for each value of q.

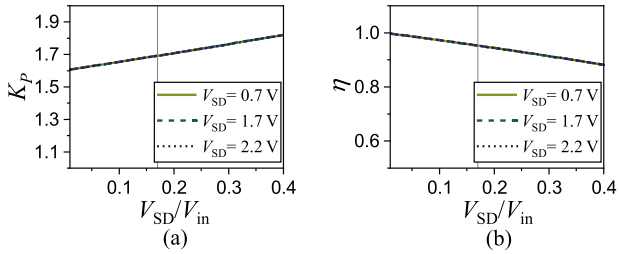

Fig. 7. (a) Power conversion capability K_P and (b) efficiency η of the cross-quadrant mode Class-E amplifiers for different $V_{\rm SD}/V_{\rm in}$. Here, $q = 1.7$. For the gray reference line, $V_{\rm SD}/V_{\rm in} = 0.17$, which is used in subsequent simulations and experiments.

of the energy storage component, i.e., inductor or capacitor, is increased). In contrast to the conventional Class-E PAs, for which the power conversion capability K_P is dramatically decreased as q is increased (namely, the inductance and/or capacitance is decreased) when $q > 1.412$[7], [25], the power conversion capability of the proposed cross-quadrant mode amplifier would not decrease but increase when the inductance/capacitance becomes small. Meanwhile, the efficiency becomes only slightly decreased [see Fig. 5(b)] as q is increased, which is acceptable for various applications.

Fig. 6 shows the voltage stress σ_V and the normalized voltage stress $\tilde{\sigma}_V$ with respect to the parameter q, respectively, for both the conventional and the proposed Class-E amplifiers. A high voltage stress may force the device to be operated at a low input voltage. In fact, one of most important roles of an amplifier or inverter in the circuit system is the output power. Since the cross-quadrant mode Class-E could have a larger K_P compared with the conventional one, it also possess higher output power when $q > 1.31$ since $P_o = K_P V_{\rm in}^2/R$. Instead of directly comparing the voltage stress for the proposed PA and the conventional one, it is fairer to utilize the normalized voltage stress when investigating the performances of the two types if amplifiers with different powers. Despite that the voltage stress σ_V for the proposed amplifier is greater than that for the conventional one when the value of q is large, the normalized voltage stress $\tilde{\sigma}_V$ of the proposed one is much smaller than that of the conventional one, indicating that our proposed cross-quadrant Class-E amplifier performs better on the cost per watt of output power.

In the subsequent designs and experiments, we chose the parameter $q = 1.7$. Now, the power conversion capability K_P is increased from 0.584 for the conventional amplifier to 1.692 for the proposed cross-quadrant one. According to (19) and (25), the power conversion capability K_P and efficiency η are functions of $V_{\rm SD}/V_{\rm in}$. Fig. 7 illustrates the power conversion capability and efficiency of the cross-quadrant mode Class-E amplifiers for different $V_{\rm SD}/V_{\rm in}$. It is clear that both the power conversion capability and efficiency depend on $V_{\rm SD}/V_{\rm in}$. When $V_{\rm SD}/V_{\rm in}$ is very small, the efficiency will be close to unity. As it is increased, the efficiency decreases proportionally. Furthermore, a tradeoff between power conversion capability and efficiency exists. One

TABLE I
PERFORMANCE COMPARISON OF CLASS-E PAS OPERATED IN THE CROSS-QUADRANT AND THE CONVENTIONAL MODES

	cross-quadrant (I, $D = 50\%$)	conventional (II, $D = 50\%$)	conventional (III, $D = 77\%$)
q	1.7	1.7	1.7
$V_{\rm in}$ [V]	10	10	10
$V_{\rm SD}$ [V]	1.7	–	–
φ	208.9°	243.3°	122.5°
θ	306.2°	–	–
$V_R/V_{\rm in}$	1.84	1.08	1.815
σ_V	4.78	3.70	7.75
$\tilde{\sigma}_V$	2.83	6.37	4.59
K_C	0.90	0.40	0.02
K_P	1.69	0.58	1.69

can select an appropriate value of $V_{\rm SD}/V_{\rm in}$ according to actual application requirements.

As mentioned in the Section I, it is theoretically possible to obtain high power conversion capability by increasing the duty cycle. However, such a method would result in a sharp increase of voltage stress, which may be impractical. Table I shows the performance comparison with the same input voltage $V_{\rm in}$ and q. Here, the duty cycle is 50% for the cases I and II, while it is increased to 77% for Case III, which yields the same normalized output power as for Case I. The normalized voltage stress $\tilde{\sigma}_V$ is 2.83 for the cross-quadrant mode, which is reduced by 55.57% and 38.34% compared with those for the cases II and III, respectively. It is evident that the proposed cross-quadrant Class-E amplifier performs best in terms of the normalized voltage stress among the three designs. Again, we shall stress that the cross-quadrant mode amplifier can achieve the same power with a lower withstand voltage of the transistor, which would reduce the cost of the device at the expense of a slight reduction in efficiency because of the reverse conduction and switching losses.

In addition, K_C reads 0.02 for Case III, which is much smaller than those for Cases I and II, meaning that the maximum switching frequency $f_{\rm max}$ of Case III is lowest among the three cases. Therefore, conventional Class-E amplifiers operating at a high duty ratio may not suitable for high-frequency applications. In contrast, K_C reads 0.90 for the proposed amplifier (Case I), which is the largest, meaning that the maximum operating frequency is the highest. Such a feature also reveals the superior

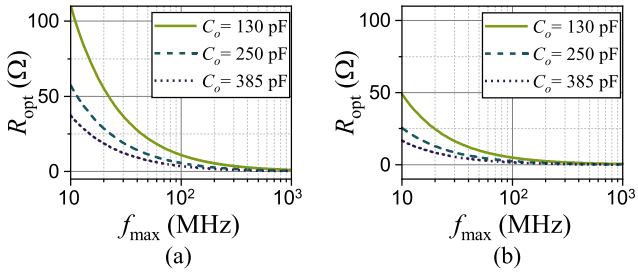

Fig. 8. Optimum load R_{opt} as functions of the maximum switching frequency f_{max} for (a) the cross-quadrant mode Class-E PA and (b) the conventional Class-E PA. Here, $q = 1.7$ and $V_{SD}/V_{in} = 0.17$.

high-frequency performance of the cross-quadrant mode Class-E amplifiers.

Fig. 8 compares the optimum load R_{opt} as functions of the maximum switching frequency f_{max} for the cross-quadrant mode Class-E PA and the conventional Class-E PA. It is evident that PAs can support a great load resistance at the same maximum switching frequency within the cross-quadrant mode. In addition, it confirms that the cross-quadrant mode Class-E amplifier has a wider frequency range compared with the conventional one.

V. Component Design and Simulation

A. Component Design Procedure

One of the critical features of the cross-quadrant mode Class-E PA is the reverse conduction state, which means that the design parameters may be affected by the reverse conduction threshold voltage of the transistor. Therefore, design procedures for conventional Class-E amplifiers may not apply to the cross-quadrant one. While different types of transistors usually have different reverse conduction voltages, we can start with a typical value of $V_{SD} = 1.7$ V to estimate the voltage and current stress in order to select a realistic GaN transistor. In addition, we usually need to recalculate the voltage and current stresses according to the actual reverse voltage of the candidate device to verify its suitability.

We can first determine the value of q according to the expected power conversion capability and efficiency. For a cross-quadrant mode Class-E inverter with given q, one can begin with a set of input specifications, i.e., the output power P_o, the switching frequency f, and the supply voltage V_{in}. Next, the design parameters p, φ, and θ are estimated with $V_{SD} = 1.7$ V according to Section III-B. As a result, we can choose proper GaN HEMT devices based on the voltage stress (27) and the current stress (29). In turn, the exact values of p, φ, and θ can be recalculated based on the actual reverse voltage V_{SD} of the device, which may not be equal to 1.7 V. Having determined these parameters, we can finally obtain the load voltage V_R and the normalized output power K_P.

As for the circuit components, the optimum resistance reads $R_{opt} = K_P V_{in}^2/P_o$ according to (1). Next, with an appropriate quality factor Q_L[1], [4], the series inductance L_1 is calculated by

$$L_1 = \frac{Q_L R}{\omega}. \tag{31}$$

Since $X/R = V_X/V_R$ with $X = \omega L_1 - 1/(\omega C_1)$, according to (16), one obtains

$$C_1 = \frac{1}{\omega^2 L_1 - \omega R V_X/V_R}. \tag{32}$$

As for the shunt capacitance across the GaN HEMT, it reads as $C = K_C/\omega R$, where $K_C = V_R/(q^2 p V_{in})$. In addition, the external shunt capacitor $C_{ext} = C - C_{oss}$ can be expressed as

$$C_{ext} = \frac{K_C}{\omega R} - C_{oss} = \frac{V_R}{\omega R q^2 p V_{in}} - C_{oss} \tag{33}$$

where the output capacitance C_{oss} of GaN HEMTs can be found in the datasheet. Finally, the dc-feed inductance L reads

$$L = \frac{pRV_{in}}{\omega V_R} \tag{34}$$

where $p = (\omega L I_R)/V_{in}$ with $I_R = V_R/R$.

TABLE II
Component Values for the Simulations

	f [MHz]	V_{in} [V]	L [μH]	C_{ext} [nF]	L_1 [μH]	C_1 [pF]	R [Ω]
Cross-quadrant	3.11	10	0.55	1.25	17.2	152.3	28
Conventional	3.11	10	1.16	0.34	24.5	99	28

B. Simulations

We have used the design parameters given in Table I for our simulation, which yield the circuit parameters as listed in Table II according to the design procedure described in Section V-A. A level 1 model of the GS61008T from GaN Systems was used in the simulation.

The simulations were performed by using LTspice circuit simulator. Fig. 9 compares the simulated voltage waveforms (viz., the gate (dashed) and drain–source voltages (blue solid) of the switches, and the load voltages) of the proposed cross-quadrant [see Fig. 9(a)] and conventional [see Fig. 9(b)] Class-E amplifiers. It is evident from Fig. 9(a) that the drain–source voltage v_{ds} for the cross-quadrant amplifier reveals three switch states, namely, ON when v_{ds} is positive, OFF when it is zero, and reverse conduction when it is negative (even though its absolute value is small). Thus, the so-called cross-quadrant operation of the transistor switch is functional. In contrast, the drain–source voltage for the conventional circuit reveals that only two switch states exist, i.e., ON when v_{ds} is positive and OFF when it is zero. Moreover, a higher output voltage v_R is achieved for the cross-quadrant mode compared with the conventional one, implying that the power conversion capability can be high by virtue of the proposed amplifier. We shall point out that the device model used in the simulation is not an ideal device, which contains a nonnegligible device parasitic capacitance. As a result, i_{ds} does not vanish during the switch-OFF period. In addition, since the ZVS condition is not satisfied for cross-quadrant mode PAs, the

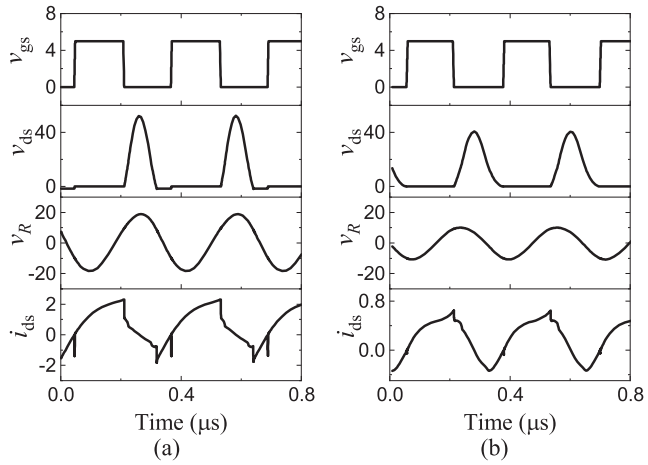

Fig. 9. Simulated waveforms of the gate voltages v_{gs}, drain–source voltages (v_{ds}) of the switches, load voltages (v_R), and the drain current i_{ds} for both the (a) cross-quadrant mode (case I) and (b) the conventional (case II) Class-E amplifiers.

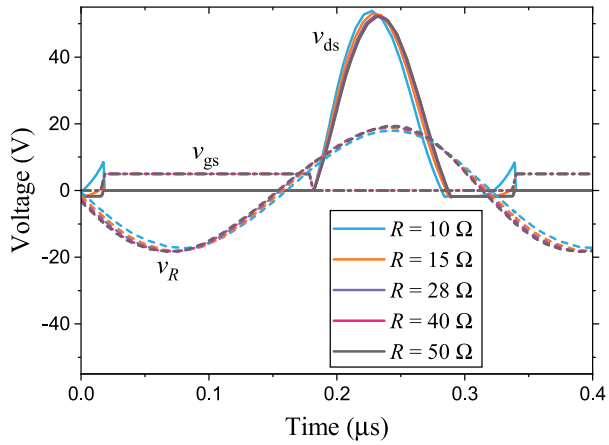

Fig. 10. Simulated waveforms of the gate (v_{gs}) and drain–source voltages (v_{ds}) of the switch and the load voltages (v_R) of the cross-quadrant mode Class-E PA for different load R.

charging and discharging process of the parasitic capacitance during the switch-on period would lead to a short current drop, as shown in Fig. 9(a).

As for performance parameters, the power conversion capability K_P^{I} of the cross-quadrant Class-E PA is 1.72, which is much greater than that of the conventional one ($K_P^{\mathrm{II}} = 0.49$). Meanwhile, the efficiency becomes slightly decreased from about 98% for the conventional amplifier to about 95% for the proposed one. The results confirm the theoretical analysis in Section IV, showing again the functionality of our proposed design. Due to the nonzero ON-resistance and voltage-dependent capacitance of the model used in the simulation, the simulated efficiency of the conventional PA is not 100%.

We performed simulations with only varying loads to test to what extent using a nonoptimal load degrades the performance of the cross-quadrant mode Class-E PA. Fig. 10 shows the simulated waveforms for various load resistance R. It is evident that the cross-quadrant mode Class-E PA is not sensitive to the load variation. When the load resistance is in the range of

TABLE III
VALUES OF COMPONENTS USED IN THE EXPERIMENTS

	Cross-quadrant (I)	Conventional (II)
Input Voltage V_{in}	10 V	10 V
Switching frequency f	3.11 MHz	3.11 MHz
Measured resistance R	27.9 Ω	27.2 Ω
DC-feed inductance L	513 nH	1.2 μH
Shunt capacitance C_{ext}	1.3 nF	313 pF
Load series capacitance C_1	153 pF	101 pF
Load series inductance L_1	17.2 μH	24.5 μH

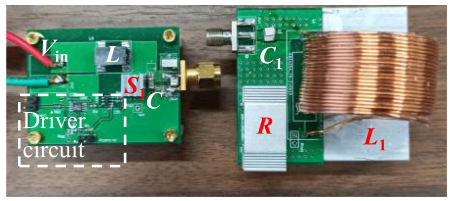

Fig. 11. Photograph of the experimental setup.

10–50 Ω, the system behaves like a constant voltage output. Changes of the drain–source voltage v_{ds} are only observable when the load is reduced to the half of the optimum load or less. In addition, when the load resistance decreases less, the reverse conduction time decreases. This means that when the load resistance is slightly smaller than the optimal load resistance, the efficiency may be slightly improved. Therefore, the efficiency of the cross-quadrant mode Class-E amplifier still has the potential to be further improved. However, when the load resistance is reduced more, the efficiency will drop due to the large switching loss.

VI. EXPERIMENTAL RESULTS AND DISCUSSIONS

We have validated the theory and design by experiments. The measured values of the component specifications for experiments are summarized in Table III. Fig. 11 shows the photograph of the experimental setups. GS61008T produced by GaN Systems was used for both the cross-quadrant mode PA (case I) and the conventional PA (case II). The same model as adopted in Section V-B is used in the simulation here. In order to sufficiently drive the gate of the GS61008T, a high-speed comparator LT1711, which is a low-side gate driver, was used to process external signal sources and to provide input signals for the gate driver LM5114.

Fig. 12(a) and (b) displays the measured waveforms for the proposed cross-quadrant mode (case I) and the conventional (case II) Class-E PAs, respectively. Again, the measured results behave similar to those of simulation results, both for the cross-quadrant and the conventional amplifiers. As illustrated in Fig. 12(a), negative drain–source voltage (brown waveform) appears in a fraction of period, meaning that such a circuit operates in the cross-quadrant mode. Meanwhile, a higher output voltage is observed for the proposed amplifier compared with the conventional one. In addition, the phase angle when the reverse conduction starts is $\theta \approx 306.3^\circ$ and the maximum voltage stress across the transistor $\sigma_V = V_{\mathrm{DSM}}/V_{\mathrm{in}} \approx 4.82$ (or

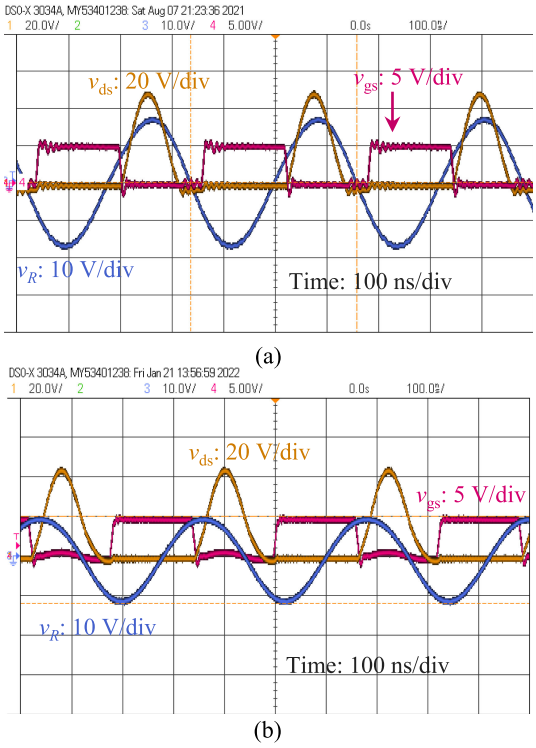

Fig. 12. Experimental waveforms of the gate (v_{gs}) and drain–source voltages (v_{ds}) of the switch, and waveforms of the load voltage (v_R) for (a) the proposed cross-quadrant (case I) and (b) the conventional (case II) Class-E amplifiers with finite dc-feed inductance, where $q = 1.7$.

TABLE IV
COMPARISON OF MEASURED RESULTS AND CALCULATED RESULTS (CASE I: CROSS-QUADRANT; CASE II: CONVENTIONAL)

	Calculated (Case I)	Measured (Case I)	Calculated (Case II)	Measured (Case II)
φ	208.9°	206.0°	243.25°	241.83°
θ	306.2°	306.3°	–	–
P_o[W]	6	6.06	2.14	2.24
P_{in}[W]	6.3	6.74	2.14	2.40
σ_V	4.78	4.82	3.70	4.42
η	95.28%	89.91%	100%	93.33%
K_P	1.692	1.69	0.584	0.61

$V_{DSM} = 48.2$ V), which also agree with the theoretical predictions given in Table I in Section III.

Table IV compares the measured results and calculated results, both for the cross-quadrant (case I) and the conventional (case II) amplifiers. It is evident that the measured results and the calculated results agree well, for both the two cases, respectively. Since the ON-resistance of the transistor is negligible and the actual values are not exactly the same as the designed values, relatively small differences exist, e.g., 5% and 7% for the efficiency η for the proposed and the conventional Class-E amplifiers, respectively. In addition, as the external capacitance C_{ext} can be small, e.g., $C_{ext} = 313$ pF in the conventional amplifier circuit, the output capacitance of the oscilloscope becomes nonnegligible, which may introduce additional discrepancy between the measured results and the theoretical results.

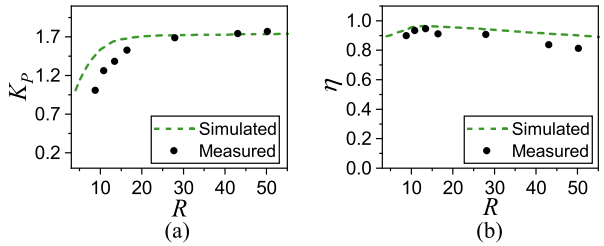

Fig. 13. (a) Power conversion capability and (b) efficiency of the proposed cross-quadrant amplifier for various R.

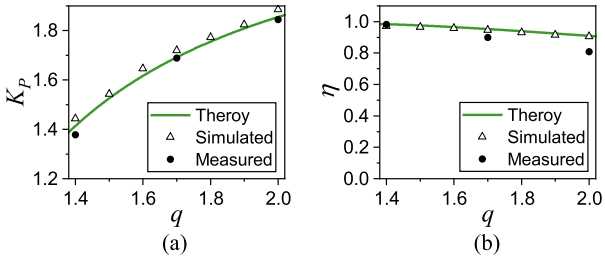

Fig. 14. (a) Power conversion capability and (b) efficiency of the proposed cross-quadrant amplifier for various q, which are obtained by the theory (solid line), the simulation (hollow marker), and the experiments (solid marker).

We have performed experiments under different load resistances to confirm the simulation results. In the experiments, the parameters given in Table III were utilized. Fig. 13 shows the power conversion capability and efficiency of the proposed cross-quadrant amplifier for various R. The experimental results agree well with the simulation. As predicted by the simulation results, the efficiency can be slightly improved when the load resistance is slightly smaller than the optimal load resistance. We shall point out that, limited by our experimental conditions, the reactance changes caused by changing the load resistance in the experiment, discrepancy appears between the measured power conversion capability K_P and the simulated results when the load resistance is small. In addition, because the switching loss of the actual switch is relatively large and the reactance cannot be guaranteed to be a constant in the experiment for varying loads, the measured efficiency and the simulated results may not be exactly the same.

Fig. 14 displays the measured power conversion capability for various design parameter $q = 1.4$, 1.7 and 2.0; also, the theoretical and simulated results are plotted as a reference. Again, the experimental results show a good agreement with the theory. We shall point out that the switch is not ideal (i.e., the actual operation of the transistor requires a certain amount of time), which yields the switching loss. Since the ON-resistance is not considered in the theoretical calculation, both the forward and reverse conduction losses may be slightly larger than the corresponding theoretical values. In addition, the larger the q, the longer the reverse conduction time, resulting in a larger discrepancy between the theory and experimental results. As a result, the discrepancy of the efficiency η between the experiments and the theory is increased as q is increased.

VII. Conclusion

In this article, we presented the analysis method for the cross-quadrant mode Class-E amplifier and showed that its power conversion capability can be enhanced. In particular, we derived a circuit model to calculate the switch voltage and current of the cross-quadrant mode Class-E PA where three operation states of transistors were involved. We demonstrated that the power conversion capability within the cross-quadrant mode is higher than that of the conventional one when the design parameter $q = (\omega\sqrt{LC})^{-1}$ (where L and C are the dc-feed inductance and the parallel capacitance of the transistor, respectively) is relatively large, with the normalized voltage stress being much smaller. Moreover, we proposed the design procedure for the GaN-based cross-quadrant mode Class-E amplifier and validated our theory and design with experiments, showing a normalized output power of 1.69 and an efficiency of near 90%. Our theory and design pave a new avenue to develop high-power Class-E amplifiers. It is expected to open a door for converters with improved power density based on Class-E PAs, which is coherent with the reduction of parameter q to increase the power conversion capability due to a reduction in the size of the choke inductor L. In the context of the emerging interest in high-frequency resonant power converters [12], [32]–[34], it also indicates that the output power and power density of such circuits can be improved with the cross-quadrant operation.

References

[1] M. K. Kazimierczuk, *RF Power Amplifiers*, 2nd ed. Hoboken, NJ, USA: Wiley, 2015.

[2] F. Raab, "Idealized operation of the class E tuned power amplifier," *IEEE Trans. Circuits Syst.*, vol. CS-24, no. 12, pp. 725–735, Dec. 1977.

[3] T. Suetsugu and M. Kazimierczuk, "Design procedure of class-E amplifier for off-nominal operation at 50% duty ratio," *IEEE Trans. Circuits Syst. I: Reg. Papers*, vol. 53, no. 7, pp. 1468–1476, Jul. 2006.

[4] M. Kazimierczuk and K. Puczko, "Exact analysis of class E tuned power amplifier at any Q and switch duty cycle," *IEEE Trans. Circuits Syst.*, vol. CS-34, no. 2, pp. 149–159, Feb. 1987.

[5] F. Raab and N. Sokal, "Transistor power losses in the class E tuned power amplifier," *IEEE J. Solid-State Circuits*, vol. SSC-13, no. 6, pp. 912–914, Dec. 1978.

[6] O. El-Aassar, M. El-Nozahi, and H. F. Ragai, "Loss mechanisms and optimum design methodology for efficient mm-waves class-E PAs," *IEEE Trans. Circuits Syst. I: Reg. Papers*, vol. 63, no. 6, pp. 773–784, Jun. 2016.

[7] M. Acar, A. J. Annema, and B. Nauta, "Analytical design equations for class-E power amplifiers," *IEEE Trans. Circuits Syst. I: Reg. Papers*, vol. 54, no. 12, pp. 2706–2717, Dec. 2007.

[8] R. Sadeghpour and A. Nabavi, "Design procedure of quasi-class-E power amplifier for low-breakdown-voltage devices," *IEEE Trans. Circuits Syst. I: Reg. Papers*, vol. 61, no. 5, pp. 1416–1428, May 2014.

[9] J. Ponte, A. Ghahremani, M. Huiskamp, A.-J. Annema, and B. Nauta, "Theory and implementation of a load-mismatch protective class-E PA system," *IEEE Trans. Circuits Syst. I: Reg. Papers*, vol. 67, no. 2, pp. 369–377, Feb. 2020.

[10] A. Ghahremani, A.-J. Annema, and B. Nauta, "Outphasing class-E power amplifiers: From theory to back-off efficiency improvement," *IEEE J. Solid-State Circuits*, vol. 53, no. 5, pp. 1374–1386, May 2018.

[11] S. Aldhaher, P. C. Luk, and J. F. Whidborne, "Tuning class E inverters applied in inductive links using saturable reactors," *IEEE Trans. Power Electron.*, vol. 29, no. 6, pp. 2969–2978, Jun. 2014.

[12] S. Aldhaher, D. C. Yates, and P. D. Mitcheson, "Load-independent class E/EF inverters and rectifiers for MHz-switching applications," *IEEE Trans. Power Electron.*, vol. 33, no. 10, pp. 8270–8287, Oct. 2018.

[13] A. Ayachit, F. Corti, A. Reatti, and M. K. Kazimierczuk, "Zero-voltage switching operation of transformer class-E inverter at any coupling coefficient," *IEEE Trans. Ind. Electron.*, vol. 66, no. 3, pp. 1809–1819, Mar. 2019.

[14] A. Grebennikov, "High-efficiency class-E power amplifier with shunt capacitance and shunt filter," *IEEE Trans. Circuits Syst. I: Reg. Papers*, vol. 63, no. 1, pp. 12–22, Jan. 2016.

[15] S. Park and J. Rivas-Davila, "Duty cycle and frequency modulations in class-E dc–dc converters for a wide range of input and output voltages," *IEEE Trans. Power Electron.*, vol. 33, no. 12, pp. 10524–10538, Dec. 2018.

[16] Y. Dou, X. Huang, Z. Ouyang, and M. A. Andersen, "Modelling and compensation design of class-E rectifier for near-resistive impedance in high-frequency power conversion," *IEEE Trans. Power Electron.*, vol. 36, no. 8, pp. 8812–8823, Aug. 2021.

[17] K. Surakitbovorn and J. M. Rivas-Davila, "A method to eliminate discrete inductors in a class-E inverter used in wireless power transfer applications," *IEEE J. Emerg. Sel. Topics Power Electron.*, vol. 8, no. 3, pp. 2167–2178, Aug. 2020.

[18] S. Assawaworrarit, X. Yu, and S. Fan, "Robust wireless power transfer using a nonlinear parity–time-symmetric circuit," *Nature*, vol. 546, no. 7658, pp. 387–390, 2017.

[19] S. Assawaworrarit and S. Fan, "Robust and efficient wireless power transfer using a switch-mode implementation of a nonlinear parity–time symmetric circuit," *Nature Electron.*, vol. 3, no. 5, pp. 273–279, 2020.

[20] J. Zhou, B. Zhang, W. Xiao, D. Qiu, and Y. Chen, "Nonlinear parity-time-symmetric model for constant efficiency wireless power transfer: Application to a drone-in-flight wireless charging platform," *IEEE Trans. Ind. Electron.*, vol. 66, no. 5, pp. 4097–4107, May 2018.

[21] T. Suetsugu and M. K. Kazimierczuk, "Off-nominal operation of class-E amplifier at any duty ratio," *IEEE Trans. Circuits Syst. I: Reg. Papers*, vol. 54, no. 6, pp. 1389–1397, Jun. 2007.

[22] R. Zhang, M. Acar, M. P. van der Heijden, M. Apostolidou, and D. M. Leenaerts, "Generalized semi-analytical design methodology of class-E outphasing power amplifier," *IEEE Trans. Circuits Syst. I: Reg. Papers*, vol. 61, no. 10, pp. 2951–2960, Oct. 2014.

[23] T. Nagashima, X. Wei, T. Suetsugu, M. K. Kazimierczuk, and H. Sekiya, "Waveform equations, output power, and power conversion efficiency for class-E inverter outside nominal operation," *IEEE Trans. Ind. Electron.*, vol. 61, no. 4, pp. 1799–1810, Apr. 2014.

[24] N. O. Sokal and A. D. Sokal, "Class E: A new class of high-efficiency tuned single-ended switching power amplifiers," *IEEE J. Solid-State Circuits*, vol. SSC-10, no. 3, pp. 168–176, Jun. 1975.

[25] A. Grebennikov and M. J. Franco, *Switchmode RF and Microwave Power Amplifiers*. New York, NY, USA: Elsevier, 2012.

[26] Y. Li, X. Ruan, L. Zhang, J. Dai, and Q. Jin, "Optimized parameters design and adaptive duty-cycle adjustment for Class E dc–dc converter with on-off control," *IEEE Trans. Power Electron.*, vol. 34, no. 8, pp. 7728–7744, Aug. 2019.

[27] J. Millan, P. Godignon, X. Perpina, A. Perez-Tomas, and J. Rebollo, "A survey of wide bandgap power semiconductor devices," *IEEE Trans. Power Electron.*, vol. 29, no. 5, pp. 2155–2163, May 2014.

[28] E. A. Jones, F. F. Wang, and D. Costinett, "Review of commercial GaN power devices and GaN-based converter design challenges," *IEEE J. Emerg. Sel. Topics Power Electron.*, vol. 4, no. 3, pp. 707–719, Mar. 2016.

[29] A. V. Grebennikov and H. Jaeger, "Class E with parallel circuit—A new challenge for high-efficiency RF and microwave power amplifiers," in *Proc. IEEE MTT-S Int. Microw. Symp*. Digest, 2002, pp. 1627–1630.

[30] Z.-L. Zhang, Z. Dong, D.-D. Hu, X.-W. Zou, and X. Ren, "Three-level gate drivers for eGaN HEMTs in resonant converters," *IEEE Trans. Power Electron.*, vol. 32, no. 7, pp. 5527–5538, Jul. 2016.

[31] Z. Zhang and Y.-F. Liu, *High Frequency MOSFET Gate Drivers: Technologies and Applications*. Bedford, MA, USA: Digital, 2017.

[32] Z. Qi *et al.*, "An accurate datasheet-based full-characteristics analytical model of GaN HEMTs for deadtime optimization," *IEEE Trans. Power Electron.*, vol. 36, no. 7, pp. 7942–7955, Jul. 2021.

[33] K. N. Surakitbovorn and J. M. Rivas-Davila, "On the optimization of a Class-E power amplifier with GaN HEMTs at megahertz operation," *IEEE Trans. Power Electron.*, vol. 35, no. 4, pp. 4009–4023, Apr. 2020.

[34] Y. Wang, O. Lucia, Z. Zhang, Y. Guan, and D. Xu, "Review of very high frequency power converters and related technologies," *IET Power Electron.*, vol. 13, no. 9, pp. 1711–1721, 2020.

Xianglin Hao (Student Member, IEEE) was born in 1998. He received the bachelor's degree in electrical engineering in 2020 from Xi'an Jiaotong University, Xi'an, China, where he is currently working toward the master's degree in electrical engineering.

His research interests include power amplifiers, non-Hermitian theory, and wireless power transmissions.

Mr. Hao is a Student Member of the CIGRE (International Council on Large Electric Systems).

Jianlong Zou received the B.Sc., M.Sc., and Ph.D. degrees in electrical engineering from Xi'an Jiaotong University, Xi'an, China, in 1999, 2002, and 2008, respectively.

In 2002, he joined the School of Electrical Engineering, Xi'an Jiaotong University, where he is currently an Associate Professor. He has good cooperation with the Hong Kong Polytechnic University, Hong Kong. In 2012, he was a Visiting Scholar with Michigan State University, East Lansing, MI, USA. His main research interests include magnetically controlled reactors, modular multilevel converters, wind generation, and nonlinear dynamics in electrical engineering.

Ke Yin received the bachelor's degree in electrical engineering from Northwestern Polytechnical University, Xi'an, China, in 2018. She is currently working toward the Ph.D. degree in electrical engineering in Xi'an Jiaotong University, Xi'an.

Her research interests include non-Hermitian electromagnetics and circuits, power electronics, wireless sensors, and wireless power transmissions.

Xikui Ma received the B.Sc. and M.Sc. degrees in electrical engineering from Xi'an Jiaotong University, Xi'an, China, in 1982 and 1985, respectively.

In 1985, he was a Lecturer with the School of Electrical Engineering, Xi'an Jiaotong University, where he became a Professor in 1992. During the academic year 1994–1995, he was a Visiting Scientist with the Department of Electrical and Computer Engineering, University of Toronto, Toronto, ON, Canada. He is the author or coauthor of more than 150 scientific and technical papers and also the author of seven books in electromagnetic fields. His current research interests include electromagnetic field theory and its applications, analytical and numerical methods in solving electromagnetic problems, chaotic dynamics and its applications in power electronics, and the applications of digital control to power electronics.

Tianyu Dong (Member, IEEE) received the B.S. and Ph.D. degrees from Xi'an Jiaotong University, Xi'an, China, in 2008 and 2014, respectively.

He is currently an Associate Professor with the School of Electrical Engineering, Xi'an Jiaotong University. From 2011 to 2013, he spent two years with the Electroactive Materials Characterization Lab, Department of Electrical Engineering, Penn State, State College, PA, USA. He is affiliated with the Center for Advanced Electromagnetism and Energy Conversion and the Interdisciplinary Center for Research and Education with an emphasis on electromagnetics, circuits, power electronics, nonlinear phenomena, and renewable energies. His research interests include theoretical, computational, and experimental research in a broad range of scientific and technical areas, including applied electromagnetics, metamaterials/metasurfaces, nanophotonics, plasmonics, energy harvesting and wireless power transfer, and other industrial relevance in electrical engineering and applied physics.